Optica Applicata, Vol. XXXIX, No. 4, 2009

Optical methods used to optimise semiconductor laser structures with tunnel injection from quantum well to InGaAs/GaAs quantum dots

WOJCIECH RUDNO-RUDZIŃSKI[1*], KRZYSZTOF RYCZKO[1], GRZEGORZ SĘK[1], MARCIN SYPEREK[1], JAN MISIEWICZ[1], EMIL-MIHAI PAVELESCU[2], CHRISTIAN GILFERT[2], JOHANN PETER REITHMAIER[2]

[1]Institute of Physics, Wrocław University of Technology, Wybrzeże Wyspiańskiego 27, 50-370 Wrocław, Poland

[2]Institute of Nanostructure Technologies and Analytics, Technische Physik, Universitaet Kassel, Heinrich-Plett-Str. 40, 34132 Kassel, Germany

[*]Corresponding author: wojciech.rudno-rudzinski@pwr.wroc.pl

We present the results of optical measurements performed on structures consisting of an InGaAs quantum well (QW), separated by a thin barrier from a layer of self-assembled InGaAs quantum dots (QDs). Such a kind of design is called a tunnel injection structure, because its functionality is based on the tunnelling of carriers from a QW to QDs, preferably with the assistance of optical phonons. In this approach, the injector QW serves as a reservoir of the carriers (due to much higher efficiency of carrier collection) and alleviates the problem of long relaxation times needed for carriers to reach the QDs ground state. In order to investigate the structures several complementary experimental techniques are applied. Photoreflectance, an absorption-like modulation spectroscopy, gives the information about the optical transitions and the electronic structure. The temperature evolution of photoluminescence allows emission efficiency and carrier losses to be determined. Photoluminescence excitation probes directly the carrier transfer from QW to the dots. The interpretation of the results is supported by the calculations in the envelope function formalism. It has been found out that the wavefunction position of the lowest lying levels depends on the QW parameters and thus different regimes of tunnelling are proposed.

Keywords: quantum dots, optical properties, lasers, tunnel injection.

1. Introduction

Tunnel injection (TI) structures [1–9] have been designed in order to improve the properties of semiconductor lasers based on self-assembled quantum dots (QDs), usually for the telecom applications. Quantum dot lasers besides having several well-known advantages, both predicted theoretically and confirmed experimentally, such as a low threshold current [10, 11], low temperature sensitivity [12–14] and wide

spectral tunability [15], suffer from the low carrier collection efficiency and from the problem of "hot carriers", *i.e.*, the majority of carriers in the system occupy excited states in the dots, states in the wetting layer (WL) and bulk-like barrier material. Hot carriers severely limit the speed of modulation in laser devices, because of the long relaxation times needed first in order to capture the carrier by the QD and second, to relax to the QD ground state (GS). This is especially important for electrons, as holes relax faster [16]. One of the approaches is to add an additional quantum well (QW) to the system, separated by a thin barrier from the QDs layer. It will act as an effective carrier reservoir, because the carrier collection of QW is much higher than in the case of QDs. Moreover, if the QW is appropriately chosen, so that its GS transition energy differs from the GS energy of QDs by the energy of lateral optical (LO) phonon, the carriers will tunnel from the QW directly to the QW GS (hence the name tunnel injection), avoiding the long relaxation processes in the QDs. Both the relaxation to the QW GS and the phonon assisted tunnelling are fast, thus the overall time needed for the carrier to reach the QDs GS is greatly reduced.

It this paper, we present investigation of the optical properties of several TI structures, consisting of $In_{0.6}Ga_{0.4}As$ QDs and $In_xGa_{1-x}As$ QW, with varying In content and well width. The electronic structure of the samples is determined by photoreflectance (PR), an absorption-like modulation spectroscopy technique which is highly sensitive to optical transitions in semiconductor heterostructures [17, 18] and which has been previously applied to other TI structures [7–9]. Numerical calculations in the framework of envelope function approximation [19] are then performed in order to interpret measured energies of optical transitions and thus to resolve the positions of levels confined in the complex quantum mechanically coupled system consisting of QW, WL and QDs. The photoluminescence (PL) spectroscopy is used to probe the emission properties of the structure investigated, finally the photoluminescence excitation (PLE) measurement is performed in order to directly confirm the transfer of carriers from QW to QDs. The results obtained from the emission-like experiments are explained in the framework of the electronic structure determined previously and conclusions on the prospects of applying TI are formulated.

2. Experiment

2.1. Structures under investigation

The samples are molecular-beam-epitaxy grown on *n* doped GaAs (100) substrate. Sample A is the reference containing the layer of $In_{0.6}Ga_{0.4}As$ QDs with the nominal thickness of 1.8 nm, surrounded by 15 nm of GaAs and embedded in AlGaAs/GaAs superlattice. Samples B, C, D and E are TI structures, in which between the 15 nm GaAs layer and the layer of QDs grown in the same conditions as in the reference structure, an additional injector QW is inserted, separated by a thin barrier from the QDs layer. In the case of sample B, this QW consists of a 15 nm thick $In_{0.2}Ga_{0.8}As$ material, and the barrier of 2 nm thick GaAs; in sample C the QW is the same and the separation layer contains 0.5 nm GaAs/1 nm $Al_{0.33}Ga_{0.66}As$/0.5 nm GaAs;

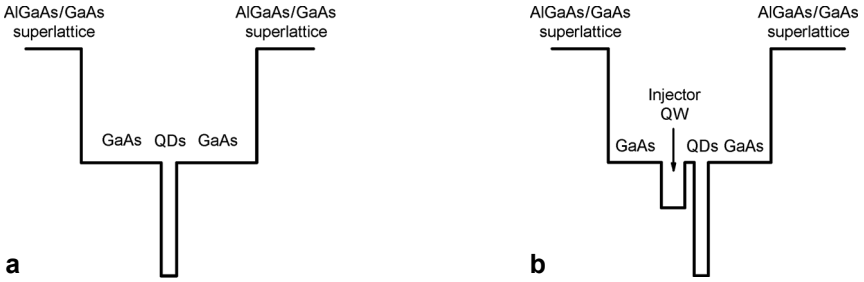

Fig. 1. Schematics of conduction band minimum for reference (**a**) and tunnel injection (**b**) samples.

samples D and E include 7 nm thick InGaAs QWs separated again by 2 nm of pure GaAs, with the In content in the well being 25% and 30%, respectively. The schematic of conduction band minimum is shown in Fig. 1.

2.2. Experimental setup

Photoreflectance is measured in a standard bright configuration setup, with the pump beam provided by the 514 nm line of an Ar^+ laser, the probe beam obtained from a tungsten halogen lamp, and detection supplied by an InGaAs photodiode combined with a 0.55 m focal length monochromator. Further details can be found in [20, 21]. The PL is measured in a similar setup, but with an InGaAs linear array used as a detector. The excitation light in the PLE experiment is provided by a tunable Ti:sapphire laser and detected also by an InGaAs linear array detector. Low temperature measurements are carried out in continuous-flow helium cryostat.

2.3. Photoreflectance results and numerical calculations

The results of room temperature PR experiment are shown in Fig. 2. The spectral range is chosen so that only transitions which are of interest in this paper (below GaAs band gap) are presented. The superlattice related part of the spectra, which does not affect the electronic structure of the active region under investigation, is out of interest in this paper. The obtained spectra can be divided into two distinct parts, depending on the origin of observed transitions. The lowest energy transition (1.05–1.1 eV) visible for all samples is attributed to the GS transition in the QDs. Its low intensity and large broadening is characteristic of PR resonances connected with self-assembled dots and is explained by the small volume of QD material and large inhomogeneous distribution of dot sizes and contents. The GS energy of QDs varies between samples, indicating some differences of average QD sizes. Since the growth of the self-assembled dots is driven by the strain, these differences are related to the different strain distribution in the samples, which may be explained by the fact the dots are grown on the top of the injector QW and barrier, which vary for each sample. Several stronger and narrower resonances visible at higher energies for the TI structures originate from the 2D part of the structure, *i.e.*, the coupled system of the injector and WL. The lowest energy state of this system shifts with the changes in the well width and content, the difference

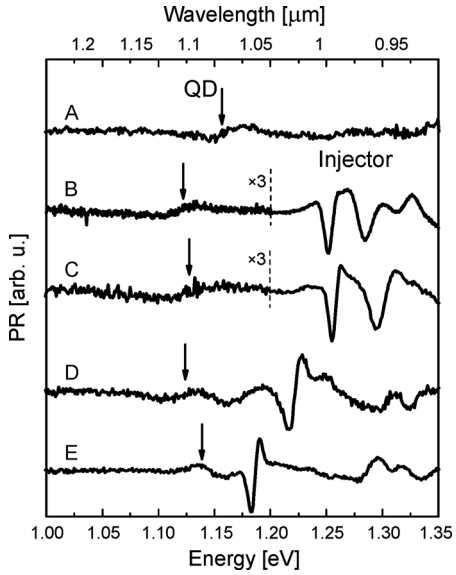

Fig. 2. PR results obtained at room temperature for all the samples. Arrows indicate QD GS transition.

in the energy between it and the QD GS ranges from over 100 meV to around 50 meV. The possibility of observing optical transitions between the excited states of the injector+WL asymmetric double QW allows better assessment of the electronic structure of the samples investigated.

In order to precisely determine the electronic structure and the positions of carrier wavefunctions of the injector+WL system, numerical calculations within the effective mass approximation in the envelope function formalism including strain [19] have been performed, with the material parameters taken after Ref. [22], with the WL thickness of three $In_{0.6}Ga_{0.4}As$ monolayers [23]. This approach allows determination of the electronic structure of QW part of the system (it does not take into account the existence of QDs). A comparison of the obtained oscillator strengths of optical transitions between light/heavy hole and electron levels and measured PR spectra is shown in Fig. 3**a**. A very good agreement between calculations (for In content in InGaAs QW lowered by 3% with respect to the nominal ones) and measurements can be clearly seen, confirming the credibility of the model applied. Figure 3**b** presents the calculated wavefunctions of carriers in the valence and conduction band wells in sample B. The lowest lying levels for two types of carriers are localized on the injector side of the barrier, whereas the higher energy states extend over both wells. The calculations for other samples yield qualitatively the same results.

Calculations of the electronic structure of 3D objects such as QDs, taking into account the realistic geometry, distribution of stress and content are complex and time consuming [24–27], especially if the QW system has to be simulated within the same approach. Because of this, the QDs layer has been modelled by changing the thickness of WL in such a way as to achieve agreement with the experimentally measured energies of two lowest energy transitions in the whole system (QD and injector+WL).

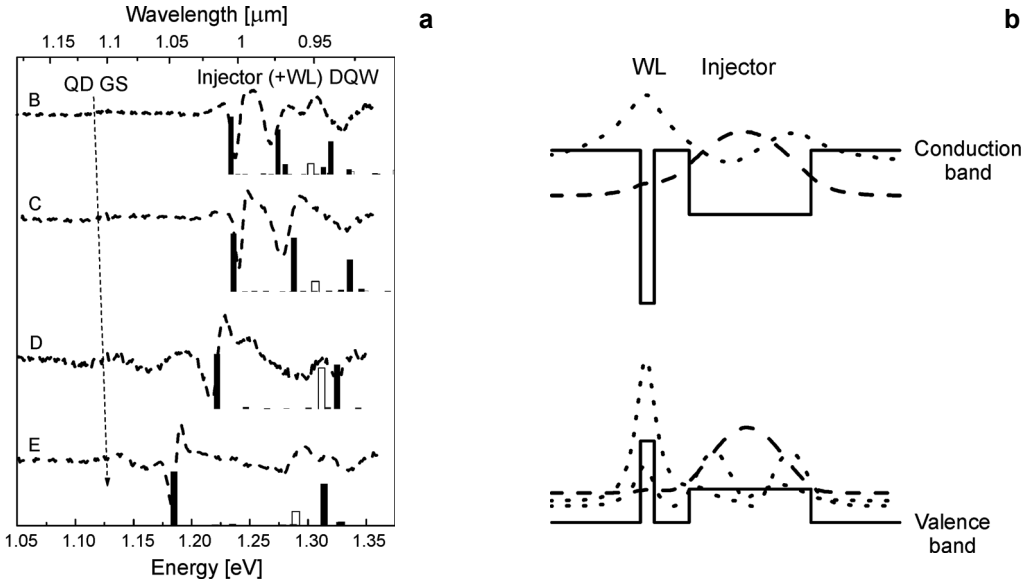

Fig. 3. Comparison of the room temperature PR spectra (dashed lines) and calculated oscillator strengths of optical transitions between heavy (full bars)/light (empty bars) hole and electron levels confined in the injector/WL system (**a**). Band structure (solid line) and wavefunctions (dashed line – GS; dotted lines – excited states) of carriers confined in sample B (**b**).

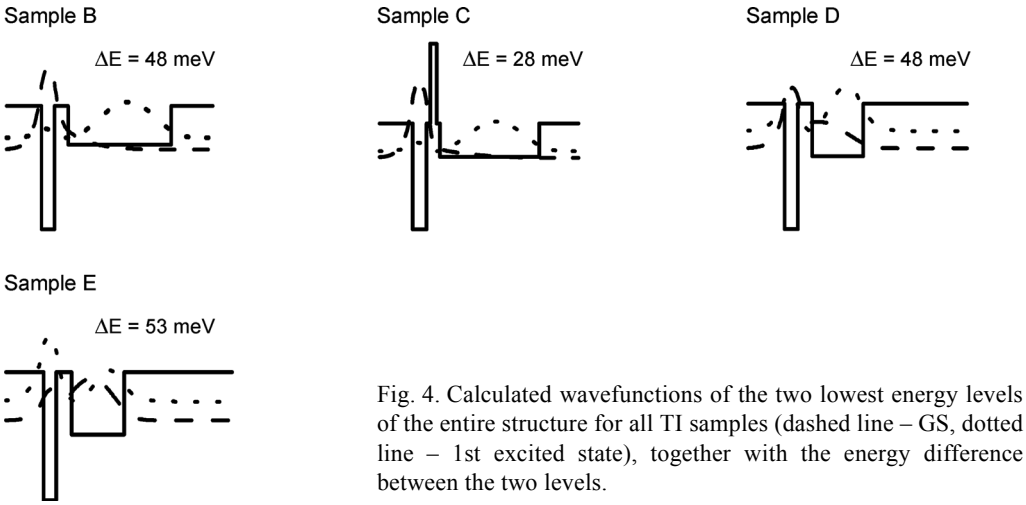

Fig. 4. Calculated wavefunctions of the two lowest energy levels of the entire structure for all TI samples (dashed line – GS, dotted line – 1st excited state), together with the energy difference between the two levels.

Although in such a model the 3D character of confinement potential is neglected (the in-plane confinement is much weaker than the one in the growth direction for this geometry of dots), some general tendencies are preserved. Since the strained band offsets for QW and QD with the same compositions are almost identical, which has been confirmed by our calculations of 3D QD potential (including the strain

distribution), the position of deeply bound electronic levels in this approximation reflects well the real situation. The localization of wavefunctions mainly depends on the depth of the confinement potential for each level, especially important being the relation between the energy of the confined level and the energy of the bottom of the injector QW. The first two electron wavefunctions obtained for all TI structures are depicted in Fig. 4, where also the energy difference between them is given. A significant difference between samples B/C (wide injector well) and D/E (narrow injector well) can be observed. While the second level for all the samples is more or less extended over both wells, the lowest energy level for samples B/C is strongly localized on the dot side of the barrier, whereas it is smeared over both wells for samples D/E, meaning that the ground states of both QDs and injector QW are in resonance with each other and the tunnelling between them may occur without phonon assistance. This is not possible in the case of samples B and C, and the best match to the GaAs LO phonon is found for sample B.

2.4. Photoluminescence and photoluminescence excitation results

In the previous paragraph, the electronic structure of the samples under investigation has been presented. Now, the influence of that structure on the emission properties will be discussed. Figure 5 shows the results of low excitation PL measurements at room temperature. First of all, the position of the peak attributed to the emission from QDs is different for all the samples, confirming the conclusion drawn from the PR results. Second, the intensity of QD-related emission varies between samples, with the strongest being the one in the reference sample A. Third, the emission from the injector QW is clearly observed only for sample E, where the difference between

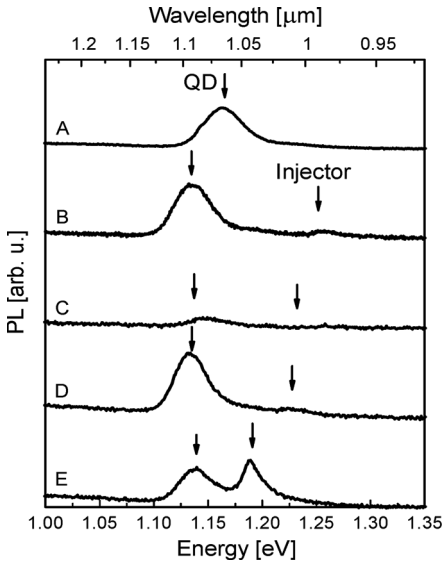

Fig. 5. Low excitation room temperature PL spectra. Arrows indicate the energies of optical transitions.

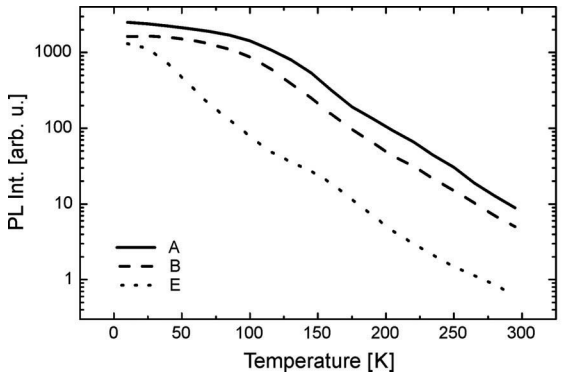

Fig. 6. Comparison of the low excitation PL quenching curves for the reference sample A and TI samples B and E.

QD GS energy and injector lowest transition energy is the smallest. It can be deduced that the addition of QW strongly affects the emission properties of the QDs, reducing its efficiency. In order to determine the specifics of the correlation between the electronic structure of the system and the QDs emission effectiveness, the PL quenching experiment has been performed (see Fig. 6).

Again, it can be seen that the intensity of emission from TI structures is at least 2–3 times lower than for the reference one. This indicates that injector QW is the source of carrier losses, mainly non-radiative (since the emission from injector QW is usually very weak). Moreover, the gradient of the PL quenching curve is much steeper for sample E, meaning that there exists a strong thermally activated back--tunnelling to the injector, where the carriers are lost. This is consistent with the fact that it is the sample in which the GS of dots and injector/WL have been found to be in resonance at room temperature. It is also the sample with the highest intensity of emission from the injector which in this case may be treated as the losses for the QDs emission.

For testing the existence of tunnelling in the samples investigated, the PLE experiment at low temperature (10 K) has been performed, with the detection window set at the ground state emission from the dots, and the excitation swept over the energy from above the GaAs barrier band gap down to the injector/WL GS. Low temperature has been necessary due to the low intensity of emission from the dots at room temperature. The results for the reference sample A have been compared to the results for the TI sample B (see Fig. 7). The results for other TI samples are similar. In order to tie the PLE signal to the electronic structure of the samples, it has been put together with the PR and high excitation PL spectra. Photoreflectance and photoluminescence spectra show several characteristic features at coinciding energies, which are attributed to the optical transitions in different parts of the structure. As can be seen, at low temperature it is possible to observe the transitions connected with the excited states

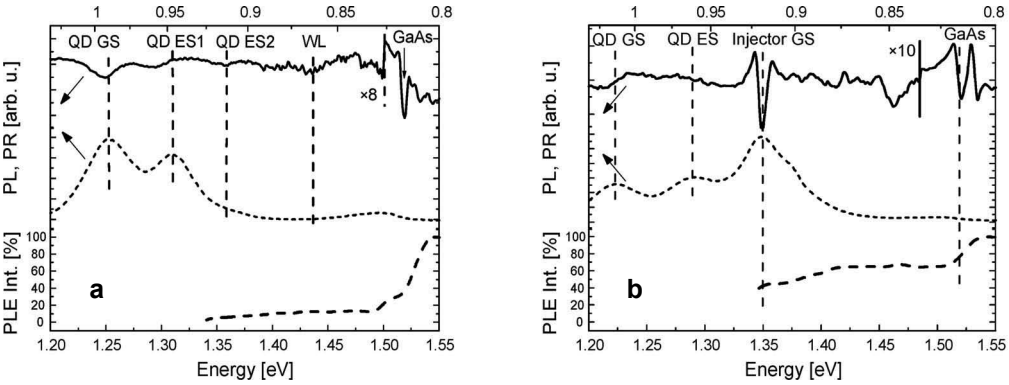

Fig. 7. Comparison of low temperature PR (solid), high excitation PL (dotted) and PLE (dashed) spectra for samples A (**a**) and B (**b**). Vertical dashed lines indicate the positions of characteristic features connected with the optical transitions. The part of the PR spectrum below GaAs band gap is multiplied for the sake of clarity.

in the QDs and also the positions of WL (reference sample) and injector/WL (sample B) related transitions are clearly visible. The PLE signal intensity in the case of reference structure drops by an order of magnitude below the GaAs band gap energy, where only the weak absorption in the thin WL QW and QDs is possible. On the other hand, the PLE signal for the sample B drops only by around 40% below the GaAs energy, and then slowly decreases, retracing the structure of transitions between levels confined in injector+WL QW system, only to drop again below the ground state of that part of the system. This clearly indicates that there is an efficient mechanism of carrier transfer from QW to QD, and since the effective barrier for each type of carriers is much higher than the thermal energy, the tunnelling through the barrier seems to be the only possible process.

3. Conclusions

We have presented the results of optical investigation of TI structures based on $In_xGa_{1-x}As$ QW and $In_{0.6}Ga_{0.4}As$ QDs. Room temperature PR results, supported by the modelling in the envelope function approximation, allowed determination of the electronic structure of this complex quantum mechanical system, consisting of QDs, injector QW and WL. It has been found that, depending on the injector QW width and content, the electron wavefunction of the lowest energy state of the entire system may be either localized on the dot side or extended over both parts of the system, constituting two different tunnelling regimes. When the GS is extended over both wells, the direct tunnelling occurs, which is not favourable for the application, since it increases the probability of carriers escaping from the dots to the injector, *i.e.*, the losses of QD emission efficiency. It is further confirmed by the emission properties of the QDs, investigated by the temperature evolution of the PL intensity. Otherwise,

when the GS wavefunction is localized in the dots, the tunnelling must be assisted by phonon, which might be beneficial from the point of view of a laser performance. Finally, the PLE experiment directly confirmed an efficient transfer of carriers from the injector QW to the dots.

Acknowledgements – This work was supported by the DeLight project no. 224366, 7th Framework Programme of the European Commission.

References

[1] BHATTACHARYA P., GHOSH S., PRADHAN S., SINGH J., ZONG-KWEI WU, URAYAMA J., KYOUNGSIK KIM, NORRIS T.B., *Carrier dynamics and high-speed modulation properties of tunnel injection InGaAs-GaAs quantum-dot lasers*, IEEE Journal of Quantum Electronics **39**(8), 2003, pp. 952–962.

[2] MI Z., FATHPOUR S., BHATTACHARYA P., *Measurement of modal gain in 1.1 μm p-doped tunnel injection InGaAs/GaAs quantum dot laser heterostructures*, Electronics Letters **41**(23), 2005, pp. 1282–1283.

[3] MI Z., BHATTACHARYA P., FATHPOUR S., *High-speed 1.3 μm tunnel injection quantum-dot lasers*, Applied Physics Letters **86**(15), 2005, p. 153109.

[4] GHOSH S., PRADHAN S., BHATTACHARYA P., *Dynamic characteristics of high-speed $In_{0.4}Ga_{0.6}As$/GaAs self-organized quantum dot lasers at room temperature*, Applied Physics Letters **81**(16), 2002, pp. 3055–3057.

[5] FATHPOUR S., BHATTACHARYA P., PRADHAN S., GHOSH S., *Linewidth enhancement factor and near--field pattern in tunnel injection $In_{0.4}Ga_{0.6}As$ self-assembled quantum dot lasers*, Electronics Letters **39**(20), 2003, pp. 1443–1445.

[6] BHATTACHARYA P., GHOSH S., *Tunnel injection $In_{0.4}Ga_{0.6}As$/GaAs quantum dot lasers with 15 GHz modulation bandwidth at room temperature*, Applied Physics Letters **80**(19), 2002, pp. 3482–3484.

[7] SĘK G., POLOCZEK P., PODEMSKI P., KUDRAWIEC R., MISIEWICZ J., SOMERS A., HEIN S., HÖFLING S., FORCHEL A., *Experimental evidence on quantum well–quantum dash energy transfer in tunnel injection structures for 1.55 μm emission*, Applied Physics Letters **90**(8), 2007, p. 081915.

[8] SĘK G., PODEMSKI P., KUDRAWIEC R., MISIEWICZ J., SOMERS A., HEIN S., HÖFLING S., REITHMAIER J.P., FORCHEL A., *Efficient energy transfer in InAs quantum dash based tunnel-injection structures at low temperatures*, Proceedings of SPIE **6481**, 2007, p. 64810F.

[9] PODEMSKI P., KUDRAWIEC R., MISIEWICZ J., SOMERS A., REITHMAIER J.P., FORCHEL A., *On the tunnel injection of excitons and free carriers from $In_{0.53}Ga_{0.47}As/In_{0.53}Ga_{0.23}Al_{0.24}As$ quantum well to $InAs/In_{0.53}Ga_{0.23}Al_{0.24}As$ quantum dashes*, Applied Physics Letters **89**(6), 2006, p. 061902.

[10] ELISEEV P.G., LI H., LIU T., NEWELL T.C., LESTER L.F., MALLOY K.J., *Ground-state emission and gain in ultralow-threshold InAs-InGaAs quantum-dot lasers*, IEEE Journal of Selected Topics in Quantum Electronics **7**, 2001, p. 135.

[11] LEDENTSOV N.N., KOVSH A.R., ZHUKOV A.E., MALEEV N.A., MIKHRIN S.S., VASIL'EV A.P., SEMENOVA E.S., MAXIMOV M.V., SHERNYAKOV YU.M., KRYZHANOVSKAYA N.V., USTINOV V.M., BIMBERG D., *High performance quantum dot lasers on GaAs substrates operating in 1.5 μm range*, Electronics Letters **39**(15), 2003, pp. 1126–1128.

[12] MAKSIMOV M.V., GORDEEV N.Y., ZAITSEV S.V., KOP'EV P.S., KOCHNEV I.V., LEDENTSOV N.N., LUNEV A.V., RUVIMOV S.S., SAKHAROV A.V., TSATSUL'NIKOV A.F., SHERNYAKOV Y.M., ALFEROV Z.I., BIMBERG D., *Quantum dot injection heterolaser with ultrahigh thermal stability of the threshold current up to 50 °C*, Semiconductors **31**(2), 1997, pp. 124–126.

[13] SHCHEKIN O.B., DEPPE D.G., *1.3 μm InAs quantum dot laser with T_o = 161 K from 0 to 80 °C*, Applied Physics Letters **80**(18), 2002, pp. 3277–3279.

[14] FATHPOUR S., MI Z., BHATTACHARYA P., KOVSH A.R., MIKHRIN S.S., KRESTNIKOV I.L., KOZHUKHOV V., LEDENTSOV N.N., *The role of Auger recombination in the temperature-dependent output characteristics ($T_0 = \infty$) of p-doped 1.3 μm quantum dot lasers*, Applied Physics Letters **85**(22), 2004, pp. 5164–5166.

[15] VARANGIS P.M., LI H., LIU G.T., NEWELL T.C., STINTZ A., FUCHS B., MALLOY K.J., LESTER L.F., *Low-threshold quantum dot lasers with 201 nm tuning range*, Electronics Letters **36**(18), 2000, pp. 1544–1545.

[16] SOSNOWSKI T.S., NORRIS T.B., JIANG H., SINGH J., KAMATH K., BHATTACHARYA P., *Rapid carrier relaxation in $In_{0.4}Ga_{0.6}As/GaAs$ quantum dots characterized by differential transmission spectroscopy*, Physical Review B **57**(16), 1998, pp. R9423–R9426.

[17] RUDNO-RUDZIŃSKI W., KUDRAWIEC R., SĘK G., MISIEWICZ J., SOMERS A., SCHWERTBERGER R., REITHMAIER J.P., FORCHEL A., *Photoreflectance investigations of InAs quantum dashes embedded in $In_{0.53}Ga_{0.47}As/In_{0.53}Ga_{0.23}Al_{0.24}As$ quantum well grown on InP substrate*, Applied Physics Letters **88**(14), 2006, p. 141915.

[18] RUDNO-RUDZIŃSKI W., SĘK G., MISIEWICZ J., LAMAS T.E., QUIVY A.A., *The formation of self--assembled InAs/GaAs quantum dots emitting at 1.3 μm followed by photoreflectance spectroscopy*, Journal of Applied Physics **101**(7), 2007, p. 073518.

[19] JONSSON B., ENG S.T., *Solving the Schrodinger equation in arbitrary quantum-well potential profiles using the transfer matrix method*, IEEE Journal of Quantum Electronics **26**(11), 1990, pp. 2025–2035.

[20] MISIEWICZ J., SITAREK P., SĘK G., KUDRAWIEC R., *Semiconductor heterostructures and device structures investigated by photoreflectance spectroscopy*, Materials Science **21**(3), 2003, pp. 263–320.

[21] SĘK G., PODEMSKI P., RUDNO-RUDZINSKI W., GUMIENNY Z., MISIEWICZ J., *Microphotoreflectance spectroscopy – a modulation technique with high spatial resolution*, Optica Applicata **37**(4), 2007, pp. 439–447.

[22] VURGAFTMAN I., MEYER J.R., RAM-MOHAN L.R., *Band parameters for III–V compound semiconductors and their alloys*, Journal of Applied Physics **89**(11), 2001, pp. 5815–5875.

[23] SEK G., POLOCZEK P., RYCZKO K., MISIEWICZ J., LÖFFLER A., REITHMAIER J. P., FORCHEL A., *Photoreflectance determination of the wetting layer thickness in the $In_xGa_{1-x}As/GaAs$ quantum dot system for a broad indium content range of 0.3–1*, Journal of Applied Physics **100**(10), 2006, p. 103529.

[24] BAHDER T.B., *Eight-band k·p model of strained zinc-blende crystals*, Physical Review B **41**(17), 1990, pp. 11992–12001.

[25] STIER O., BIMBERG D., *Modeling of strained quantum wires using eight-band k·p theory*, Physical Review B **55**(12), 1997, pp. 7726–7732.

[26] GRUNDMANN M., STIER O., BIMBERG D., *InAs/GaAs pyramidal quantum dots: Strain distribution, optical phonons, and electronic structure*, Physical Review B **52**(16), 1995, pp. 11969–11981.

[27] LI L.H., PATRIARCHE G., CHAUVIN N., RIDHA P., ROSSETTI M., ANDRZEJEWSKI J., SĘK G., MISIEWICZ J., FIORE A., *Controlling the aspect ratio of quantum dots: From columnar dots to quantum rods*, IEEE Journal of Selected Topics in Quantum Electronics **14**(4), 2008, pp. 1204–1213.

Received June 23, 2009
in revised form August 26, 2009